Electrochimica Acta xxx (2009) xxx–xxx

Contents lists available at ScienceDirect

Electrochimica Acta

journal homepage: www.elsevier.com/locate/electacta

Probing the electrochemical behaviour of SWCNT–cobalt nanoparticles and their electrocatalytic activities towards the detection of nitrite at acidic and physiological pH conditions

Abolanle S. Adekunle [a], Jeseelan Pillay [a], Kenneth I. Ozoemena [a,b,*,1]

[a] Molecular and Nanomaterials Electrochemistry Laboratory, Department of Chemistry, University of Pretoria, Pretoria 0002, South Africa
[b] Energy and Processes Unit, Materials Science and Manufacturing, Council for Scientific and Industrial Research (CSIR), Pretoria, Pretoria 0001, South Africa

ARTICLE INFO

Article history:
Received 26 November 2008
Received in revised form 20 February 2009
Accepted 28 February 2009
Available online xxx

Keywords:
Single-walled carbon nanotubes
Cobalt nanoparticles
Electron transfer behaviour
Impedance spectroscopy
Adsorption
Nitrite detection

ABSTRACT

The electrochemical decoration of edge plane pyrolytic graphite electrode (EPPGE) with cobalt and cobalt oxide nanoparticles integrated with and without single-walled carbon nanotubes (SWCNTs) is described. Successful modification of the electrodes was confirmed by field emission scanning electron microscopy (FESEM), AFM and EDX techniques. The electron transfer behaviour of the modified electrodes was investigated in $[Fe(CN)6]^{3-/4-}$ redox probe using cyclic voltammetry (CV) and electrochemical impedance spectroscopy (EIS) and discussed. The study showed that cobalt nanoparticles modified electrodes exhibit faster electron transfer behaviour than their oxides. The catalytic rate constant (K) obtained at the EPPGE–SWCNT–Co for nitrite at pH 7.4 and 3.0 are approximately the same ($\sim 3 \times 10^4$ cm^3 mol^{-1} s^{-1}) while the limits of detection (LoD = $3.3\delta/m$) are in the μM order. From the adsorption stripping voltammetry, the electrochemical adsorption equilibrium constant β was estimated as $(13.0 \pm 0.1) \times 10^3$ M^{-1} at pH 7.4 and $(56.7 \pm 0.1) \times 10^3$ M^{-1} at pH 3.0 while the free energy change (ΔG°) due to the adsorption was estimated as −6.36 and −10.00 kJ mol^{-1} for nitrite at pH 7.4 and 3.0, respectively.

1. Introduction

One of the disadvantages of the employing bare electrode in electroanalysis is their sluggish electron transfer behaviour. The sluggish electron transfer behaviour at the bare electrode can be improved upon by surface modification with electron transfer mediators such as carbon nanotubes and redox active metal nanoparticle catalysts. Because of their unique structure, electrical and mechanical properties [1], there have been reports on applications of carbon nanotubes (CNTs) in nanoscale hydrodynamics [2], field emission devices [3], catalysis of redox reactions [4–6], nanoelectronics [7], hydrogen storage [8], electrochemical capacitors [9,10] and electrochemical sensors [11]. Several authors have reported the excellent electrocatalytic properties of nanotubes towards the electrocatalytic response of different molecules and bio-molecules such as hydrazine [12], NADH [13], dopamine [14], nitric oxide [15], ascorbic acid [5] and hydrogen peroxide [16]. Thus, carbon nanotubes-modified electrodes have shown interesting catalytic properties toward electrochemical processes. Recently there have been renewed interests in the preparation and characterization of carbon nanotubes/metal (CNT–M) hybrid systems as electroactive material for sensor [17–22] and catalysts [23,24] among which Co, Ni and Fe are important members of mixed-valence transition metal which have proven to have excellent properties in electrocatalysis. Studies have shown that carbon nanotubes provided a large surface for metal deposition on electrodes and thus provided a synergistic relationship for an improve electron transfer between the base electrode and the CNT–M hybrids [25–27]. However, the extent and the mechanism for the electron transfer of the CNT–M and carbon nanotubes–metal oxide (CNT–MO) modified electrodes are not clearly understood. Studies using Co and cobalt oxides (CoO) decorated electrodes for biological and environmental sensing have been reported [28–32]. Electrodes decorated with CoO nanoparticles without CNTs for sensing properties have also been studied [33,34]. However, few studies using CNT–Co modified electrodes have been carried out [35–39], prepared mainly by chemical reduction processes rather than by electrodeposition. For example, Yang et al. [37] used chemically prepared cobalt haxacyanofferate nanoparticles–CNT–chitosan modified electrode (CoNP–CNT–CHIT) for glucose detection. Recently, Shen et al. [38] reported Pt–Co nanoparticles supported on single-walled carbon nanotubes (SWCNTs–Pt–Co) obtained via chemical process for methanol oxidation. Also, Zhao et al. [39] made the composite by chemical reduction of cobalt salt in CNT solution and the electrode, containing other metals as composite shows good electrocatalysis towards methanol oxidation. More importantly,

* Corresponding author. Tel.: +27 12 841 3664; fax: +27 12 841 2135.
E-mail address: kozoemena@csir.co.za (K.I. Ozoemena).
[1] ISE member.

0013-4686/$ – see front matter © 2009 Elsevier Ltd. All rights reserved.
doi:10.1016/j.electacta.2009.02.102

reports on the electron transfer behaviour of Co nanoparticles or cobalt nanoparticles integrated with single-walled carbon nanotubes (SWCNT–Co) as hybrid material for electrochemical sensing are limited. Hence, developing simple and reliable methods for fabrication of SWCNT–Co hybrid systems as sensing platform is of importance.

Nitrite ion is important as it is commonly used as an additive in some foods [40,41]. It can be formed as a result of the degradation of some fertilizers and corrosion inhibitor [42]. Apart from being one of the major components of waste water from nuclear power production [43,44], involved in corrosion [45] and the bacterial process known as the nitrogen cycle [46], nitrite also plays important physiological roles in the form of NO, for example, as a neurotransmitter, and an immune system mediator [40]. Nitrite promotes corrosion when dissolved in water and is also classified as an environmentally hazardous species because of its toxicity [47]. The ions can interact with amines to form carcinogenic nitrosamines [48]. Oxidation of nitrite on bare electrode has been reported to be accompanied with a high over potential [49]. The use of chemically modified electrodes (CMEs) has been developed to decrease the overpotential for nitrite oxidation. This work presents the electron transfer (ET) properties of edge plane pyrolytic graphite electrode modified with SWCNTs and Co nanoparticles (EPPGE–SWCNT–Co) and its corresponding oxides (EPPGE–SWCNT–CoO). The ET property was investigated using cyclic voltammetry (CV) and electrochemical impedance spectroscopy (EIS). Since nitrite exists mainly as nitric oxide in acidic medium [49], the electrocatalytic oxidation of nitrite at acidic (pH 3.0) and physiological pH (pH 7.4) was also examined.

2. Experimental

2.1. Materials and reagents

Single-walled carbon nanotubes (SWCNTs) were purchased from Aldrich and digested by subjecting it to harsh acid conditions following a known procedure [50] for the purposes of transforming the SWCNT into shorter, uncapped nanotubes bearing mainly carboxylic functional groups. $Co(NO_3)_2{\cdot}6H_2O$, $NaNO_2$ and other reagents were of analytical grade and used as supplied without further purification. Phosphate buffer solutions (PBS) at various pHs were prepared with appropriate amounts of $NaH_2PO_4{\cdot}2H_2O$ and $Na_2HPO4{\cdot}2H_2O$, and the pH adjusted with 0.1 M H_3PO_4 or NaOH. Ultra pure water of resistivity 18.2 MΩ cm was obtained from a Milli-Q Water System (Millipore Corp., Bedford, MA, USA) and was used throughout for the preparation of solutions.

2.2. Equipment and procedure

The edge plane pyrolytic graphite (EPPG) plate was purchase from Le Carbone, Sussex, UK and was constructed locally by placing it in a Teflon tube, extended outside with a copper wire to make electrical contact with the electrochemical equipment. Field emission scanning electron microscopy (FESEM) images were obtained from JEOL JSM 5800 LV (Japan) while the energy dispersive x-ray spectra were obtained from NORAN VANTAGE (USA). AFM experiments were performed with AFM 5100 System (Agilent Technologies, USA) using an acoustic mode AFM scanner interfaced with a Picoscan (scan range 1.25 μm in x–y and 2.322 μm in z). Silicon type PPP-NCH-20 (Nanosensors®) of thickness 4.0 ± 1.0 μm, length 125 ± 10 μm, width 30 ± 7.5 μm, spring constants 10–130 N m^{-1}, resonant frequencies of 204–497 kHz and tip height of 10–15 μm were used. All images (256 samples/line × 256 lines) were taken in air at room temperature and at scan rates 0.9–1.0 lines s^{-1}.

Electrochemical experiments were carried out using an Autolab Potentiostat PGSTAT 302 (Eco Chemie, Utrecht, The Netherlands) driven by the GPES software version 4.9. Electrochemical impedance spectroscopy measurements were performed with an Autolab Frequency Response Analyser (FRA) software between 0.1 Hz and 10 kHz using a 5 mV rms sinusoidal modulation with a solution of 5 mM of $K_4Fe(CN)_6$ and a 5 mM $K_3Fe(CN)_6$ (1:1) mixture in phosphate buffer solution of pH 7.0 and at the equilibrium potential ($E_{1/2}$) of the $[Fe(CN)_6]^{3-/4-}$ (0.3 V vs Ag|AgCl, sat'd KCl). A Ag|AgCl, sat'd KCl and platinum wire were used as reference and counter electrodes, respectively. The unmodified and modified EPPGE served as the working electrodes. A bench top pH/ISE ORION meter, model 420A, was used for pH measurements. All solutions were de-aerated by bubbling nitrogen prior to each electrochemical experiment. All experiments were performed at 25 ± 1 °C.

2.3. Electrode modification and pretreatments

EPPGE surface was cleaned by gentle polishing in aqueous slurry of alumina nanopowder (Sigma–Aldrich) on a SiC-emery paper and then to a mirror finish on a Buehler felt pad. The electrode was then subjected to ultrasonic vibration in absolute ethanol to remove residual alumina particles that might have been trapped at the surface. EPPGE–SWCNT was prepared by a drop-dry method. About 20 μL drop of the SWCNTs/DMF solution (7 mg acidified SWCNTs in 1 mL DMF) was dropped on the bare EPPGE and dried in an oven at 50 °C for about 2 min. Cobalt nanoparticles were electrodeposited onto the EPPGE–SWCNT (herein abbreviated as EPPGE–SWCNT–Co) using chronoamperometry technique in 5 mM $Co(NO_3)_2{\cdot}6H_2O$ solution at a fixed potential of −2.0 V for 5 min, a similar procedures adopted by others for the deposition of metal particles on electrodes [51–54]. The EPPGE–SWCNT–CoO electrode was obtained by immersing the EPPGE–SWCNT–Co in 0.1 M PBS (pH 7.0) and repetitively scanning (20 scans) between 1.5 and −0.8 V potential window at a scan rate of 100 mV s^{-1} [52,53].

3. Results and discussion

3.1. Comparative FESEM, AFM images EDX spectra

Fig. 1 shows the comparative scanning electron microscopy (SEM) images of the EPPGE, EPPGE–SWCNT, EPPGE–SWCNT–Co and EPPGE–SWCNT–CoO.

Upon electrodeposition of Co nanoparticles, EPPGE–SWCNT–Co modified electrode was formed (Fig. 1c). There is high dispersion of Co nanoparticles, possibly made due to the strong electrostatic interactions between the Co^{2+} ions in solution and the COO^- charge of the SWCNTs on the electrode surface. The Co nanoparticles form a porous and high electroactive material on the electrode surface but with several interstitial spaces or voids. Repetitive cycling (20 scans) of EPPGE–SWCNT–Co electrode in 0.1 M phosphate buffer solution, PBS (pH 7.0) gave EPPGE–SWCNT–CoO modified electrode in which the cobalt particles formed a thick amorphous film (Fig. 1d) with little voids. AFM topographic heights (not shown) increased from 14 nm for bare substrate to 80 nm on integrating with SWCNTs and finally to 120 nm on incorporation with cobalt or its oxides. Salimi et al. [34,57] employed similar method of electrode decoration with cobalt oxide nanoparticles and observed particles agglomeration with sizes ranging from 100 to 600 nm. As evident from the cross-sections (Fig. 1g and h), the particle sizes are in the 8–30 nm range, suggesting some agglomeration of the nanoparticles.

Fig. 2 is the EDX profile of the electrodes. The EPPGE electrode (A) was purely carbon (~100%) as would be expected for pure graphite surface. The presence of oxygen peaks in the EPPGE–SWCNT (B)

Please cite this article in press as: A.S. Adekunle, et al., Probing the electrochemical behaviour of SWCNT–cobalt nanoparticles and their electrocatalytic activities towards the detection of nitrite at acidic and physiological pH conditions, Electrochim. Acta (2009), doi:10.1016/j.electacta.2009.02.102

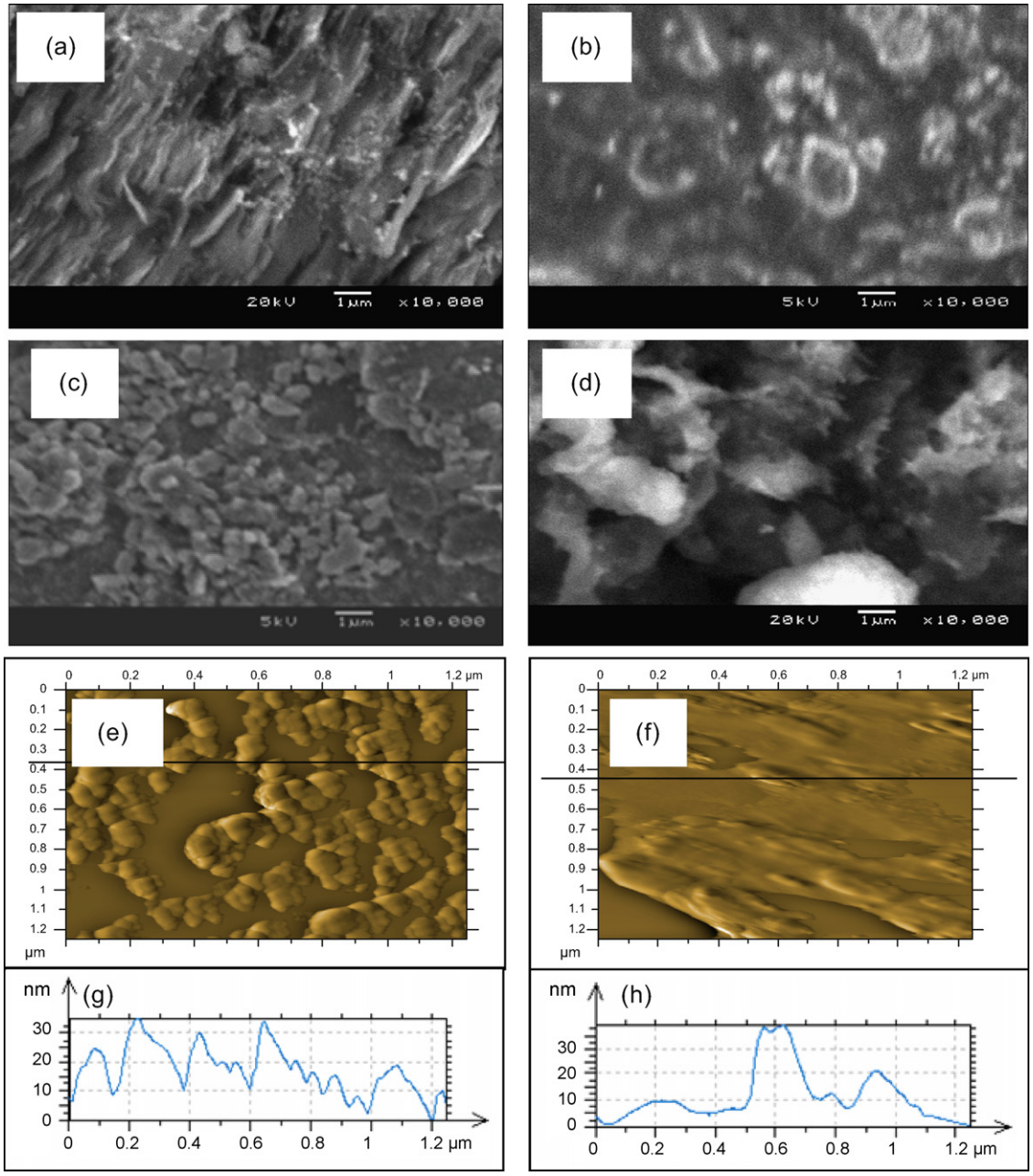

Fig. 1. FESEM of (a) EPPGE, (b) EPPGE–SWCNT, (c) EPPGE–SWCNT–Co, and (d) EPPGE–SWCNT–CoO. (e) and (f) are the AFM topography images for the EPPGE–SWCNT–Co and the EPPGE–SWCNT–CoO while (g) and (h) are their respective cross-sections.

is an indication of the successful modification of the SWCNT to the acid derivatives SWCNT–COOH while the sulphur peak can be attributed to the sulphuric acid used during treatment.

EPPG–SWCNT–CoO (C) showed the presence of Co and oxygen peaks with very pronounced intensity implying that the electrode was successfully modified with CoO nanoparticles. The occurrence of P and Na peaks in the EDX of EPPGE–SWCNT–CoO may be attributed to the sodium phosphate buffer solution used for the electrode treatment.

3.2. Comparative electrochemical characterization

Comparative current response (not shown) of bare EPPGE, EPPGE–Co, EPPGE–CoO, EPPGE–SWCNT, EPPGE–SWCNT–Co and EPPG–SWCNT–CoO in PBS (pH 7.0) was investigated. From the cyclic voltammograms (not shown), the anodic peak at 0.68 V and its corresponding cathodic peak at around 0.46 V are attributed to Co(II)/Co(III) which has been reported to be at 0.7–0.8 V (vs SCE) [54–56] in an acidic medium. The anodic peak at 0.68 V vs Ag|AgCl, sat'd KCl (~0.64 V vs SCE) is close to 0.6 V vs SCE reported by Salimi et al. [57] and was attributed to the formation of Co_3O_4 through the reaction below:

$$3Co(OH)_2 + 2OH^- \rightarrow Co_3O_4 + 4H_2O + 2e^- \quad (1)$$

Another anodic peak was observed at around +1.0 V, also observed by others [57] at 0.95 V and assigned to COOH formation as a result of oxidation of $Co(OH)_2$ or the Co_3O_4 as represented by the equations below.

$$Co(OH)_2 + OH^- \rightarrow CoOOH + H_2O + e^- \quad (2)$$

$$Co_3O_4 + H_2O + OH^- \rightarrow 3CoOOH + e^- \quad (3)$$

Please cite this article in press as: A.S. Adekunle, et al., Probing the electrochemical behaviour of SWCNT–cobalt nanoparticles and their electrocatalytic activities towards the detection of nitrite at acidic and physiological pH conditions, Electrochim. Acta (2009), doi:10.1016/j.electacta.2009.02.102

Sunohara et al. [58] reported the peak at potential >1.0 V (vs Ag|AgCl) and attributed it to the Co_2O_3/Co_3O_4 redox process. A cathodic peak was also observed at ca 0.72 V and is attributed to the reduction of CoOOH to $Co(OH)_2$ or Co_3O_4. Peak at around −0.2 V (vs Ag|AgCl, sat'd KCl) is due to Co^{2+}/Co redox process, similar to that observed by others [57] at around −0.1 V (vs SCE) on a cobalt oxide nanoparticles modified glassy carbon electrode. The current responses of these electrodes increase in this order: EPPGE–SWCNT–Co > EPPGE–SWCNT–CoO > EPPGE–Co > EPPGE–CoO > EPPGE–SWCNT > bare EPPGE.

The result indicates that: (i) deposition of SWCNT on the bare EPPGE enhances its electron transfer since SWCNTs could be acting as the conducting electrical nanowires for the flow of electrons; (ii) enhanced current response was observed when the cobalt nanoparticles were integrated with the SWCNTs, implying a positive synergistic behaviour between these two nanomaterials; and (iii) the SWCNT–Co modified electrodes gave higher current responses with decreased peak-to-peak separation potential ($\Delta Ep = 0.23$ V) compared with those without SWCNT ($\Delta E = 0.32$ V). It is therefore reasonable to suggest that SWCNTs enhance the electrochemical response of the modified electrodes by serving as the conducting nanowires for electron transfer between the Co nanoparticles and the underlying EPPGE.

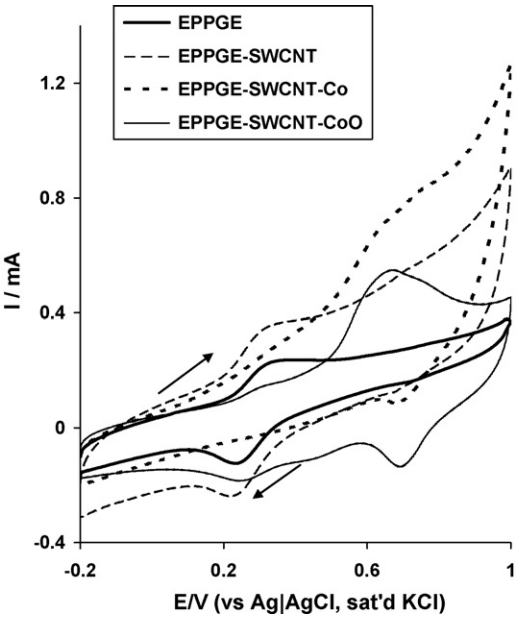

Fig. 3. Typical examples of some cyclic voltammetric evolutions of the electrodes in 5 mM $[Fe(CN)_6]^{4-}/[Fe(CN)_6]^{3-}$ solution (PBS pH 7.0). Scan rate = 50 mV s^{-1}.

3.3. Comparative electron transport properties

The aim of this experiment was to explore the extent to which the modifiers allow the electron transport between $Fe(CN)_6]^{4-}/[Fe(CN)_6]^{3-}$ redox probe and the base EPPGE. The CV experiments were performed in 5 mM $Fe(CN)_6]^{4-}/[Fe(CN)_6]^{3-}$ solution (in PBS pH 7.0). The peaks in the 0–0.4 V region is due to the $Fe(CN)_6]^{4-}/[Fe(CN)_6]^{3-}$ redox couple while the one at the 0.4–1.0 V region is ascribed to the Co(II)/Co(III) redox process (Fig. 3).

For further understanding of the electronic behaviour of the SWCNT and SWCNT–Co modified electrodes (EPPGE–SWCNT, EPPGE–SWCNT–Co, EPPGE–SWCNT–CoO), we carried out EIS study in $Fe(CN)_6]^{4-}/[Fe(CN)_6]^{3-}$ solution at the equilibrium potential of the redox couple ($E_{1/2}$ of 0.3 V) as seen in Fig. 4. The impedance technique is a very sensitive technique which gives insight into the mechanism of the electron transport between the electrode|electrolyte interface. The Nyquist plots for some of the electrodes are presented in Fig. 4a.

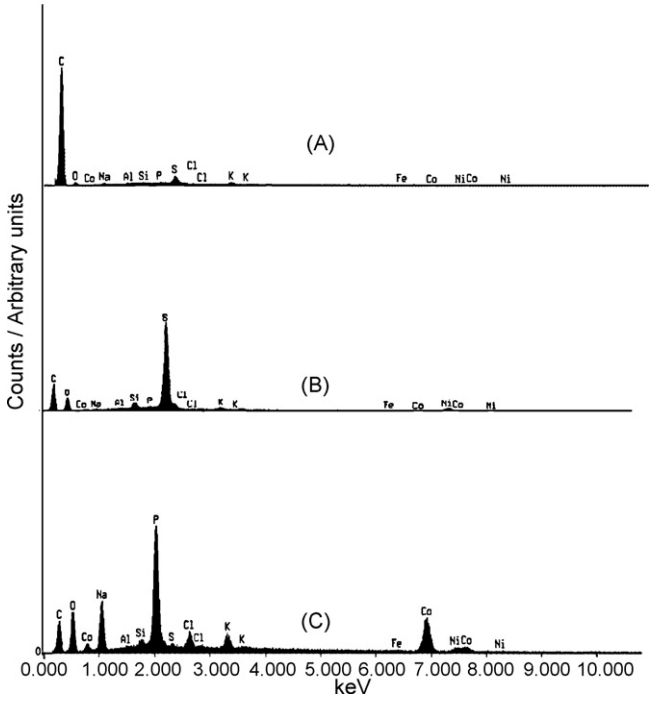

Fig. 2. EDX spectra of (A) EPPGE, (B) EPPGE–SWCNT, and (C) EPPGE–SWCNT–CoO.

All the obtained spectra were first subjected to the Kramers–Kronig (K–K) test. The main essence of the K–K test is simply to check whether the measured impedance spectra comply with the assumptions of the well known K–K transformation, viz (i) that the impedimetric response is only related to the excitation signal; (ii) that the impedimetric response is linear (or the perturbation is small, e.g., <10 mV, for non-linear systems; (iii) that the system does not change with time, say due to ageing, temperature changes, non-equilibrium conditions, etc; and (iv) that the system is finite for all values of ω, including zero and infinity [59,60]. Failure of the K–K test, signified by a large value of pseudo χ^2 is usually an indication that no good fit can be obtained using the electrical equivalent circuits methods. It should be noted that aside from visual inspection of goodness of the fitting lines, two accurate ways to establish how well the modeling functions reproduce the experimental data sets are the relative error estimates (in %) and chi-square functions (χ^2) [61], which is the sum of squares of the relative residuals (i.e., sum of the real and imaginary χ^2), easily obtained from the K–K test. The EIS data was satisfactorily fitted with the modified Dolin–Ershler equivalent circuit model (Fig. 4b) [62], judged by the values of the pseudo χ^2 and relative % errors (Table 1) as well as the goodness of fit (Fig. 4a) wherein the true capacitance (C_{dl}) is replaced by the constant phase element (CPE). In this model the R_s is the solution/electrolyte resistance, R_{ct} represents the charge transfer resistance, C_{film} describes the high pseudocapacitive nature of the system while CPE describes porous nature of the electrode. The passive layer formed by the EPPGE–SWCNT–CoO leads to an insulated surface which could be responsible for the high R_{ct} value. It is evident from this study that the EPPGE–SWCNT–Co has the least R_{ct} value indicating faster electron transport. Circuit 4b description is different from the circuit used in earlier report involving SWCNT/Ni [22] probably because of the porous nature of the EPPGE which alters its electronic properties with use [63].

Please cite this article in press as: A.S. Adekunle, et al., Probing the electrochemical behaviour of SWCNT–cobalt nanoparticles and their electrocatalytic activities towards the detection of nitrite at acidic and physiological pH conditions, Electrochim. Acta (2009), doi:10.1016/j.electacta.2009.02.102

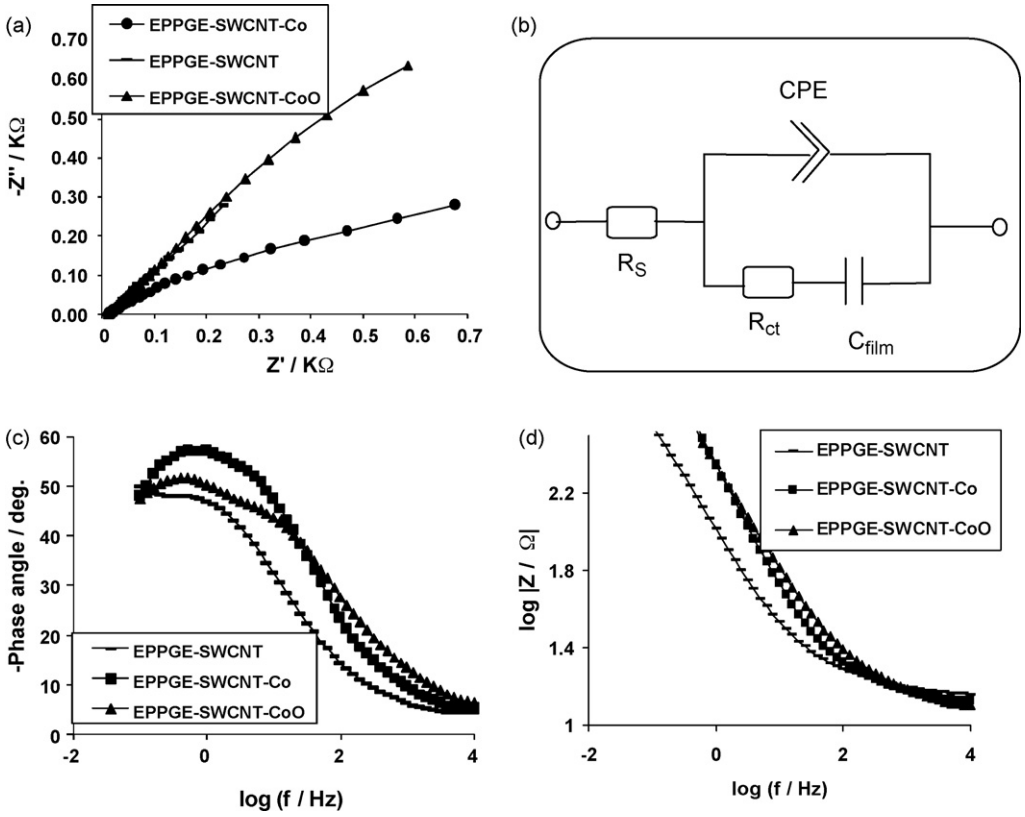

Fig. 4. (a) Typical Nyquist plots of some of the electrodes obtained in 5 mM $[Fe(CN)6]^{4-}$/$[Fe(CN)6]^{3-}$ solution (PBS pH 7.0) at fixed potential of 0.30 V vs Ag|AgCl sat'd KCl. The square data points are experimental while the solid lines in the spectra represent non-linear squares fits. (b) Represents the circuit used in the fitting of the EIS data. (c) and (d) are the Bode plots obtained for the electrodes, showing the plots of (−phase angle (deg.) vs log(f/Hz)) and log $|Z/\Omega|$ vs log(f/Hz).

The relatively low R_{ct} for the SWCNT–Co indicates faster electron transport compared to the other electrodes, possibly as a result of the porous and the high electroactive surface area of the electrode which allows for easy contact between the electrolyte and the base EPPGE. The high R_{ct} value for the SWCNT–CoO is attributed to the formation of a thick cobalt oxide nanoparticles films which increase in thickness as the number of scans increases during modification. The impedance of CPE is defined as

$$Z_{CPE} = \frac{1}{[Q(j\omega)^n]} \quad (4)$$

where Q is the frequency-independent constant relating to the surface electroactive properties, ω is the radial frequency, the exponent n arises from the slope of $\log Z$ vs $\log f$ (and has values $-1 \leq n \leq 1$). If n=0, the CPE behaves as a pure resistor; $n = 1$, CPE behaves as a pure capacitor, $n = -1$ CPE behaves as an inductor; while $n = 0.5$ corresponds to Warburg impedance (Z_w) which is associated with the domain of mass transport control arising from the diffusion of ions to and from the electrode|solution interface. Generally speaking, CPE has been known to occur via several factors notably (i) the nature of the electrode (e.g., roughness and polycrystallinity), (ii) distribution of the relaxation times due to heterogeneities existing at the electrode|electrolyte interface, (iii) porosity and (iv) dynamic disorder associated with diffusion [64]. Thus, the n values in Table 1 of approximately 0.6 may be interpreted as a near-Warburg system involving the diffusion of ions to and from the electrode|solution interface.

From the plot of $\log|Z|$ vs $\log f$, Fig. 4d, the higher slope value (−0.65, $R^2 = 0.9997$ for EPPGE–SWCNT–Co) compared with −0.57, $R^2 = 0.9991$ for EPPGE–SWCNT–CoO and −0.52, $R^2 = 0.9988$ for EPPGE–SWCNT suggests the more capacitive nature of EPPGE–SWCNT–Co than its oxide and the SWCNT counterparts. As has elegantly been described by the recent work of Orazem and Tribollet [65], time-constant (or frequency) dispersions leading to CPE behaviour occur as a result of distribution of time constants along either the area of the electrode surface (involving a 2-dimensional aspect of the electrode) or along the axis normal to the electrode surface (involving a 3-dimensional surface). Importantly, a 2-D distribution presents itself as an ideal RC behaviour, meaning that impedance measurements are very useful in distinguishing whether the observed global CPE behaviour is due to a 2-D distribution, from a 3-D distribution, or from a combined 2-D and 3-D distributions. We may therefore conclude that the observed impedimetric behaviour of the electrodes is a combination of 2-D and 3-D distributions.

Table 1
Impedance data obtained for the EPPGE modified electrodes in 5 mM $[Fe(CN)_6]^{4-}$/$[Fe(CN)_6]^{3-}$ solution (PBS pH 7.0) at 0.30 V vs Ag|AgCl sat'd KCl. All values were obtained from the fitted impedance spectra after several iterations using the circuits. Note that the values in parentheses are percent errors of data fitting.

Electrodes	Impedimetric parameters					
	R_s (Ω cm²)	CPE (mF)	n	R_{ct} (Ω cm²)	C (μF)	Pseudo χ^2
EPPGE–SWCNT	3.23 (0.13)	3.56 (0.64)	0.56 (0.61)	12.93 (2.55)	135.00 (8.98)	2.55×10^{-3}
EPPGE–SWCNT–Co	2.93 (0.67)	1.32 (1.38)	0.62 (1.08)	8.72 (2.55)	75. 80 (12.37)	7.50×10^{-5}
EPPGE–SWCNT–CoO	1.24 (0.10)	1.56 (0.77)	0.57 (0.56)	17.96 (1.38)	22. 07 (18.68)	9.50×10^{-4}

Please cite this article in press as: A.S. Adekunle, et al., Probing the electrochemical behaviour of SWCNT–cobalt nanoparticles and their electrocatalytic activities towards the detection of nitrite at acidic and physiological pH conditions, Electrochim. Acta (2009), doi:10.1016/j.electacta.2009.02.102

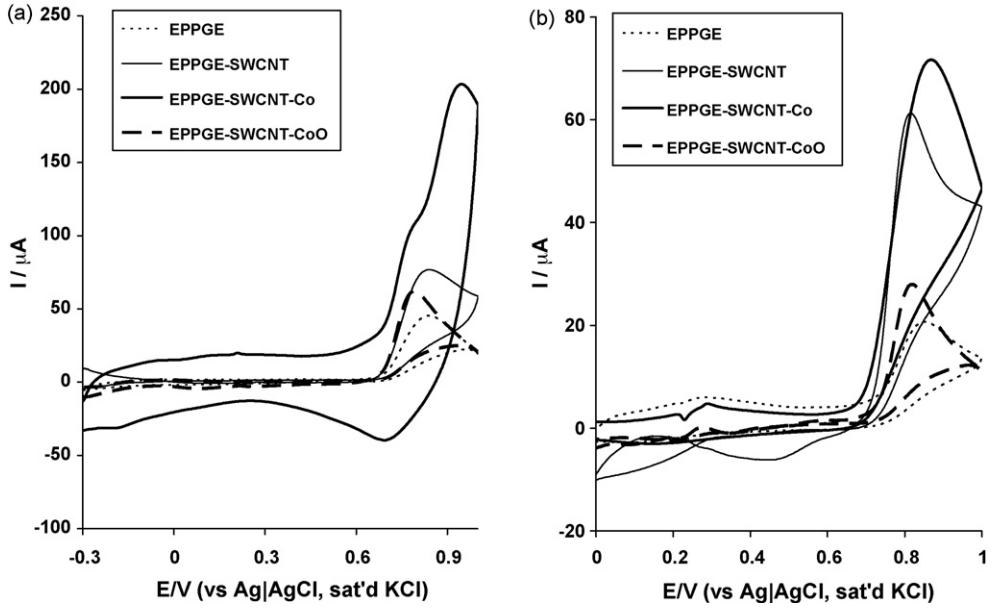

Fig. 5. Comparative current response (after background current subtraction) of the EPPGE, EPPGE–SWCNT, EPPGE–SWCNT–Co and EPPGE–SWCNT–CoO in (a) 1 mM nitrite solution in pH 7.4 PBS and (b) 1 mM nitrite solution in pH 3.0 PBS. Scan rate = 25 mV s^{-1}.

From the other type of Bode plot (i.e., −phase angle vs log *f*, Fig. 4c) the phase angles were 65° for EPPGE–SWCNT–Co compared with the EPPGE–SWCNT–CoO (51°) and EPPGE–SWCNT (48°), which are less than the 90° expected of an ideal capacitive behaviour confirming the presence of CPE and pseudocapacitive nature of these electrodes.

3.4. Electrocatalytic oxidation of nitrite in neutral and acidic pH

Fig. 5 presents the current responses of the modified electrodes in 10^{-3} M NO_2^- in PBS pH 7.4 and pH 3.0, respectively. The nitrite exists as nitrite ion (NO_2^-) in pH 7.4 PBS and at slightly acidic pH, the nitrite ion disproportionate to produce the neutral nitric oxide (NO) [49], which has a very short life time especially in an air saturated condition. Thus, the solution under the acidic pH was prepared fresh, with nitrogen purged, de-aerated phosphate buffer solution before analysis.

The current response of the EPPGE–SWCNT–Co towards nitrite at pH 7.4 was approximately 3 folds higher than the other electrodes (Fig. 5a) with slightly lower onset potentials (0.78 V). At pH 3.0 the EPPGE–SWCNT–Co exhibits faster catalysis compared to EPPGE–Co (less positive potential, ~100 mV lower than Co electrodes without SWCNTs), but the current response was almost the same. Cobalt modified electrode have been reported to give enhanced response towards electro-oxidation of nitrite on graphite substrate [58,66,67] and on gold modified electrode [68,69]. It is evident from Fig. 5a that the oxidation potential was lower with high current response on the EPPGE–SWCNT–Co nanoparticles modified electrode prepared

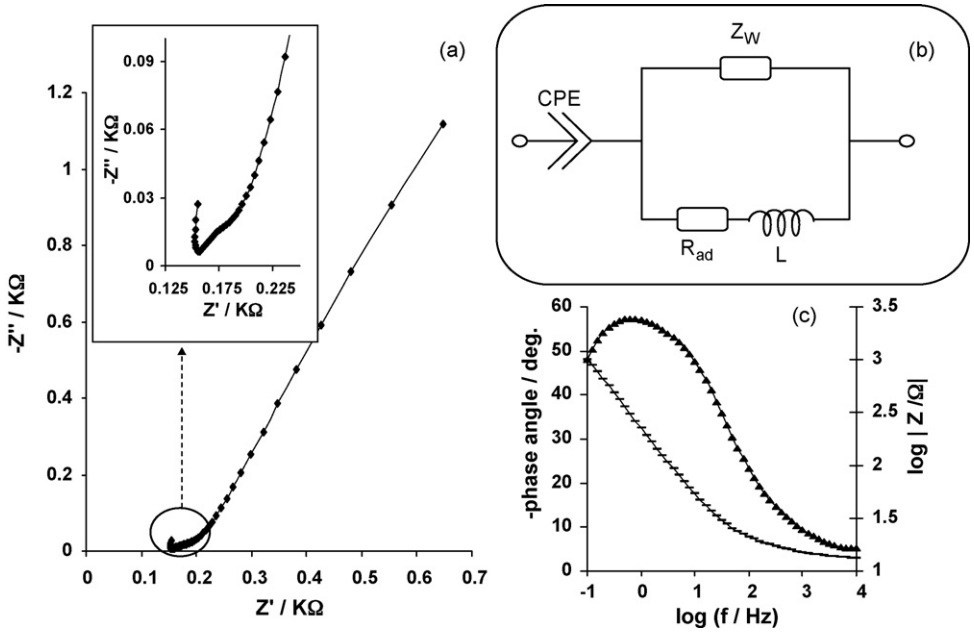

Fig. 6. (a) Typical Nyquist plots of some electrodes in 1 mM nitrite solution (PBS pH 7.4) at fixed potential of 0.80 V vs Ag|AgCl sat'd KCl. Inset is the enlarged portion of the high frequency region (b) Represents the circuit used in the fitting of the EIS data in (a). (c) Bode plot obtained for EPPGE–SWCNT–Co showing the plot of −phase angle (deg.) vs log(*f*/Hz).

Please cite this article in press as: A.S. Adekunle, et al., Probing the electrochemical behaviour of SWCNT–cobalt nanoparticles and their electrocatalytic activities towards the detection of nitrite at acidic and physiological pH conditions, Electrochim. Acta (2009), doi:10.1016/j.electacta.2009.02.102

by electrodeposition. The better electro-oxidation reaction of the SWCNT modified electrodes especially the EPPGE–SWCNT–Co, can be attributed to the SWCNT itself acting as an electrical conducting nanowire which enhances electron transport between the base electrode and the analyte. Since EPPGE–SWCNT–Co proved to be the best electrode towards nitrite oxidation at the pH conditions investigated, all further studies were carried out with it, unless otherwise stated.

3.5. Electrochemical impedance studies

Fig. 6a presents the Nyquist plots for the electrochemical impedance (EIS) data obtained at the electrodes studied during the electrocatalytic oxidation of nitrite (in pH 7.4 PBS) at a fixed potential of 0.8 V vs Ag|AgCl, sat'd KCl.

The results obtained for the oxidation of the analyte at pH 3.0 PBS follow similar trend (not shown). A circuit model (Fig. 6b) which incorporates the constant phase element and an inductor L, yielded satisfactory results with acceptable values of pseudo χ^2 and % error values (Table 2). This suggests that there may be adsorption of the oxidation product on the electrodes. Thus, the CPE with n values of 0.73 and 0.87 suggest pseudocapacitive properties occurring at the electrode|solution interface.

In electrocatalytic reactions, it is known that inductive behaviour takes place when the Faradaic current is governed by the occupation of an intermediate state [70–72]. The inductive behaviour can be attributed to factors such (1) instrumental artefacts, or (2) the inductance of the electrode, or (3) the inductance of the connecting wires (Research Solutions and Resources available online at: http://www.consultrsr.com/resources/eis/induct2.htm). We ruled out factors (1) and (3) by repeating the experiment several times but same results were obtained. R_{ad} (adsorption or partial charge transfer resistance) and L are well known as electrical elements associated with the adsorption of reaction intermediate(s) [70–72], clearly indicating the involvement of reaction intermediate products in the overall electro-oxidative process. This adsorption phenomenon is expected since CNT used as part of the electrode modifier, is known for adsorption properties because of their high surface area [27]. This is the first time the adsorption associated with nitrite oxidation is proven by EIS measurement.

3.6. Effect of varying scan rate

Cyclic voltammetric experiments were carried out with the EPPGE–SWCNT–Co to establish the impact of scan rate (ν) at constant concentration (1 mM) of nitrite at pH 7.4 and 3.0 solutions. In cases, we observed a shift in potential with increase in scan rate (not shown). From the Randles–Sevčik equation for an anodic oxidation process [73] (Eq. (5)):

$$I_p = 3.01 \times 10^5\, n[(1-\alpha)n_\alpha]^{1/2} A C_b D^{1/2} \nu^{1/2} \quad (5)$$

where n is the number of electron transfer, α is the electron transfer coefficient, n_α is the number of electrons involved in the rate-determining step, A is the electrode area, C_b is nitrite bulk concentration (1 mM) and D is the diffusion coefficient of nitrite, the plot of the peak current (I_p) against the square root of scan rate ($\nu^{1/2}$) (Fig. 7) for scan rate ranging from 25 to 200 mV s^{-1}, gave a linear relationship (R^2 = 0.9969 for nitrite oxidation at pH 7.4 with approximately zero intercept, confirming a diffusion-controlled process). However, at higher scan rate (>200 mV s^{-1}), plot of the peak current (I_p) against the square root of scan rate ($\nu^{1/2}$) gave a straight line (R^2 = 0.996) with a negative intercept suggesting that at higher scan rates the reaction is not totally diffusion controlled. This result supports the earlier discussed adsorption of intermediate products under the EIS study.

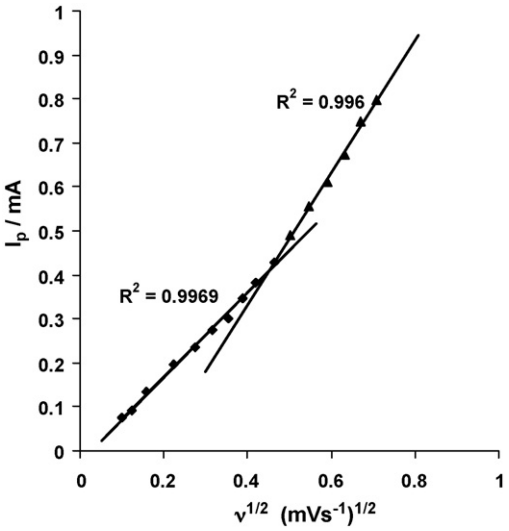

Fig. 7. Plot of peak current (I_p) vs square root of scan rate ($\nu^{1/2}$) for EPPGE–SWCNT–Co in 0.1 M pH 7.4 PBS containing 10^{-3} M nitrite.

Using Tafel equation (Eq. (6)) for a totally irreversible-diffusion-controlled process [73], the linear relationship between the peaks potential E_p and the log ν (not shown) confirms the chemical irreversibility of nitrite electrocatalytic oxidation process.

$$Ep = \frac{b}{2} \log \nu + \text{const.} \quad (6)$$

From Eq. (6), b = Tafel slope = $2.303RT/(1-\alpha)nF$ where R, T and F have their usual meaning, n is the number of exchange electrons and α is the electron transfer coefficient. Assuming n = 2 for nitrite, the value of electron transfer coefficient (α) was obtained from Eq. (6) as 0.72 for nitrite at pH 7.4.

Secondly, a Tafel slope of about 240 and 214 mV/Decade at pH 7.4 and 3.0, respectively, implies a strong binding of reactants or intermediates on the electrode surface, or reactions occurring within a porous electrode structure [69]. The value agreed with 0.73 reported for cobalt phthalocyanide modified electrode for the oxidation of nitrite [68]. The minimum α value should be 0.5 for all standard reaction mechanism [74]. α values at approximately 0.5 indicate that there is an equal probability that the reaction activated transition state can form either products or reactants [69]. Thus, α value larger than this indicates a more favoured reaction mechanism [74], which may explain why the electrocatalytic oxidation of nitrite to its oxidation product was more favoured on the EPPGE–SWCNT–Co electrode compared with the bare EPPGE.

3.7. Electroanalysis of nitrite at neutral and acidic pH

Chronoamperometric experiment was carried out by setting the peak potential at which the analyte was best catalysed. The chronoamperogram (Fig. 8) was obtained by adding different aliquots of the nitrite solution. Using Eq. (7) [57]:

$$\frac{I_{cat}}{I_l} = \pi^{1/2}(kC_0 t)^{1/2} \quad (7)$$

where I_{cat} and I_l are the currents in the presence and absence of nitrite. K is the catalytic rate constant, C_0 is the bulk concentration and t is the elapsed time. From the plot of I_{cat}/I_l vs $t^{1/2}$ (not shown) the catalytic rate constant K for EPPGE–SWCNT–Co in pH 7.4 and 3.0 PBS containing 10^{-3} M NO_2^- are 0.32 and 0.34 $\times$ 10^5 cm^3 mol^{-1} s^{-1}, respectively. Our results are approximately same as the 2.75×10^3 M^{-1} s^{-1} (or 2.75×10^6 cm^3 mol^{-1} s^{-1}) reported by Ojani et al. [75] for the electrocatalytic reduction of nitrite on carbon paste electrode modified with ferricyanide but lower than

Please cite this article in press as: A.S. Adekunle, et al., Probing the electrochemical behaviour of SWCNT–cobalt nanoparticles and their electrocatalytic activities towards the detection of nitrite at acidic and physiological pH conditions, Electrochim. Acta (2009), doi:10.1016/j.electacta.2009.02.102

Table 2
Impedance data obtained for the modified EPPGE–SWCNT–Co electrodes in 10^{-3} M NO_2^- (in PBS pH 7.4 and 3.0) at 0.80 V vs Ag|AgCl sat'd KCl. Note that the values in parentheses are percent errors of data fitting.

Electrodes	Impedimetric parameters					
	CPE (mF)	n	$10^6 Z_w$ (cm^2)	$10^6 L$ (H cm^2)	R_{ad} (Ω cm^2)	Pseudo χ^2
EPPGE–SWCNT–Co (at pH 7.4 PBS)	0.12 (1.93)	0.73 (1.33)	1.48 (0.94)	80. 6 (1.77)	38.37 (0.22)	1.02×10^{-4}
EPPGE–SWCNT–Co (at pH 3.0 PBS)	0.91 (14.84)	0.87 (6.42)	3.21 (3.35)	2877.93 (7.21)	73.36 (1.72)	3.49×10^{-5}

7×10^5 M^{-1} s^{-1} (or 7×10^8 cm^3 mol^{-1} s^{-1}) reported by Trofimova et al. [76] for catalytic oxidation of nitric oxide and nitrite by water-soluble manganese(III) meso-tetrakis(*N*-methylpyridinium-4-yl) porphyrin (Mn(III)(4-TMPyP) on indium–tin oxide (ITO) electrode in pH 7.4 phosphate buffer solutions. The difference in the magnitude of *K* could be due to the different electrode modifier and their interaction with the nitrite molecules.

Similarly, the plot of I_p vs [NO_2^-] gave the sensitivity values which are (0.2496 ± 0.0036) $\mu A\,\mu M^{-1}$ NO_2^- at pH 7.4 and (0.0316 ± 0.0007) $\mu A\,\mu M^{-1}$ for NO at pH 3.0. The limits of detection (LoD = $3.3\delta/m$ [77] where δ is the relative standard deviation of the intercept of the *y*-coordinates from the line of best fit, and *m* the slope of the same line) are 5.61 and 8.03 μM for nitrite and nitric oxide, respectively. Our result is in the same μM detection range reported for nitrite and nitric oxide on electropolymerizable iron(III) and cobalt(II) complexes on glassy carbon electrode [78] or indium(III) hexacyanoferate(III) (InHCF) on glassy carbon electrode [79]. We are not aware of any literature on the electro-oxidation of nitrite using the type of electrode reported in this work. The sensitivity obtained in this study could be due to the ability of SWCNTs to function as efficient conducting species for the catalytic cobalt nanoparticles. From Langmuir adsorption isotherm theory (Eq. (8)) [80], the plot of the ratio of concentration [nitrite] and the catalytic current I_{cat} ([nitrite]/I_{cat}) against concentration [nitrite] (not shown) gave a straight line which can be interpreted as an adsorption-controlled electrochemical process.

$$\frac{[\text{Nitrite}]}{I_{cat}} = \frac{I}{\beta I_{max}} + \frac{[\text{Nitrite}]}{I_{max}} \tag{8}$$

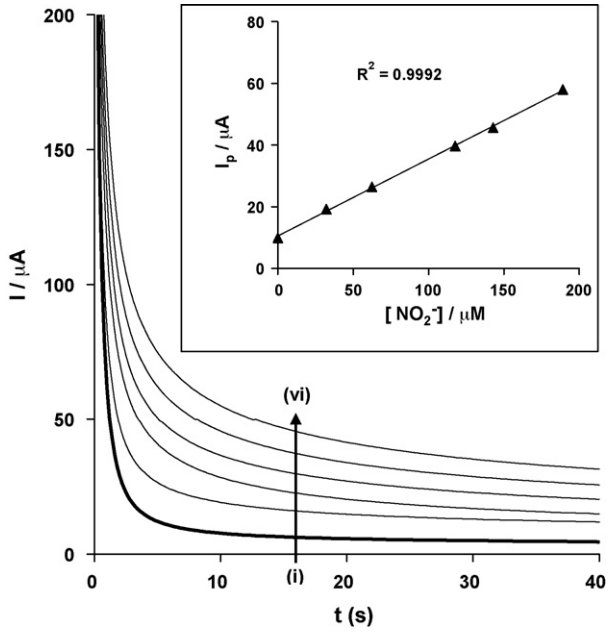

Fig. 8. Typical examples of chronoamperogram obtained for EPPGE–SWCNT–Co in phosphate buffer solution (pH 7.4) containing different concentrations of nitrite (0.0, 32.3, 62.5, 118.0, 143.0, and 189.0 μM (i to vi)). Inset is typical plot of current response vs nitrite concentration.

The adsorption equilibrium constant for the EPPGE–SWCNT–Co was estimated as β $(9.94 \pm 0.05) \times 10^3$ M^{-1} and $(4.80 \pm 0.02) \times 10^3$ M^{-1} for NO_2^- and NO. Thus, the Gibbs free energy change due to adsorption was estimated as −22.81 and −21.00 kJ mol^{-1} using Eq. (9).

$$\Delta G^\circ = -RT \ln \beta. \tag{9}$$

From the scan rate study and other studies, adsorption of the analyte on our electrode was evident. Further probe into the adsorptive properties of nitrite was carried out using the adsorption stripping voltammetry. The linear sweep voltammetric evolutions (not shown) of EPPGE–SWCNT–Co in PBS containing different aliquots of nitrite was obtained. Plot of I_p vs [NO_2^-] gave LoD values of 8.4 and 11.6 μM for nitrite at pH 7.4 and 3.0. Using Eqs. (7) and (8) above, the adsorption equilibrium constant β was estimated as $(13.02 \pm 0.03) \times 10^3$ M^{-1} and $(56.7 \pm 0.01) \times 10^3$ M^{-1} for nitrite at pH 7.4 and 3.0. Thus, the Gibbs energy change due to the adsorption was estimated as −6.36 and −10.00 kJ mol^{-1} for pH 7.4 and 3.0, respectively.

From our result, adsorption of NO_2^- and NO on our electrode followed about the same kinetics based on the insignificant difference in their standard free energy of adsorption (ΔG°). This is not unexpected since the tendency for the two analytes to interchange is very high, and they both give nitrate (NO_3^-) as their final oxidation product. The adsorption stripping voltammetry technique seems to be more viable for nitrite analysis on our electrode system since the high negative ΔG° further confirms the strong adsorption of nitrite. From the above discussion, and based on the previous reports on the mechanism of NO_3^- electro-oxidation at modified electrodes [81], we assume that the electrocatalytic response of NO_3^- at EPPGE–SWCNT–Co in aqueous solutions follows a similar mechanism:

$$[\text{SWCNT–Co}]_{film} + H_2O \rightarrow [\text{SWCNT–Co}^{2+}]_{film(aq)} + e^- \tag{10}$$

$$[\text{SWCNT–Co}^{2+}]_{film} + NO_2^- \rightleftarrows [\text{SWCNT–Co}^{2+}\text{–}(NO_2^-)]_{adduct} \tag{11}$$

$$[\text{SWCNT–Co}^{2+}\text{–}(NO_2^-)]_{adduct} \rightleftarrows [\text{SWCNT–Co}^{3+}]_{film} + NO_2 + e^-(\text{slow}) \tag{12}$$

$$2NO_2 + H_2O \rightleftarrows 2H^+ + NO_3^- + NO_2^- \tag{13}$$

$$NO_2^- + H_2O \rightarrow 2H^+ + NO_3^- + 2e^- \tag{14}$$

$$[\text{SWCNT–Co}^{3+}]_{film} + e^- \rightarrow [\text{SWCNT–Co}^{2+}]_{film} \tag{15}$$

The nitrite ion interact with the SWCNT-confined Co(II) film forming an adduct (Eq. (11)). This step represents the adsorption process. Eq. (12) is assumed to be the rate-determining step which is a one-electron process. The oxidation of the Co(II) to Co(III) simultaneously leads to the generation of the nitrogen dioxide. The formation of the NO_2 (Eq. (12)) is followed by its disproportionation to give nitrite and nitrate (Eqs. (13) and (14)). Co(III) is reduced to regenerate the Co(II) (Eq. (15)).

4. Conclusion

This study showed that the Co nanoparticle modified electrodes exhibited faster electron transfer behaviour in $[Fe(CN)_6]^{3-/4-}$ redox

Please cite this article in press as: A.S. Adekunle, et al., Probing the electrochemical behaviour of SWCNT–cobalt nanoparticles and their electrocatalytic activities towards the detection of nitrite at acidic and physiological pH conditions, Electrochim. Acta (2009), doi:10.1016/j.electacta.2009.02.102

probe than their corresponding nano-oxides. The high charge transfer resistance of the cobalt oxide modified electrodes have been attributed to surface passivation and low surface active materials. EPPGE–SWCNT–Co has the fastest electron transport, aided by the electrical conducting single-walled carbon nanotubes which form a synergistic effect with the cobalt nanoparticles. The detection and the electrocatalytic oxidation of nitrite were successful on all the electrodes studied. EPPGE–SWCNT–Co gave the highest current response, and at lower potential compared with other electrodes investigated. The electrocatalytic oxidation of nitrite on the electrode followed adsorption-controlled electrochemical process with complex impedance behaviour. There is no significant difference in the standard free energy change (ΔG°) due to adsorption, suggesting that the adsorption of NO_2^- and NO on the EPPGE–SWCNT–Co followed about the same mechanism. The study showed that, using this kind of electrode system for sensing and analytical application requires a special caution since the adsorptive nature of the electrode may have an effect on its sensing properties towards the analyte.

Acknowledgements

This project is supported by the University of Pretoria and the NRF under the "*unlocking the future programme*" (GUN # 2073666), *Research Infrastructure Support Programme* (RISP) Grants (GUN # 65305) and the "*Nanotechnology Flagship Programme*" (NFP) grants (GUN # 68338). A.S.A. thanks the NRF and DST/MINTEK (NIC) for PhD bursary and scholarship. Sincere gratitude to Andrew for acquiring the FESEM and Pretorious for the in-house fabrication of the EPPGE.

References

[1] C.M. Liu, H. Cao, Y. Li, H. Xu, Y. Zhang, Carbon 44 (2006) 2919.
[2] M. Majumder, N. Chopra, R. Andrews, B.J. Hinds, Nature 438 (2005) 930.
[3] R.H. Baughman, A.A. Zakhidov, W.A. de Heer, Science 297 (2002) 787.
[4] J.J. Davis, R.J. Coles, H. Allen, O. Hill, J. Electroanal. Chem. 440 (1997) 279.
[5] H. Luo, Z. Shi, N. Li, Z. Gu, Q. Zhuang, Anal. Chem. 73 (2001) 915.
[6] J.M. Nugent, K.S.V. Santhanam, A. Rubio, P.M. Ajayan, Nano Lett. 1 (2001) 87.
[7] S.J. Tans, A.R.M. Verschueren, C. Dekker, Nature 393 (1998) 49.
[8] C. Liu, Y.Y. Fan, M. Liu, H.T. Cong, H.M. Cheng, M.S. Dresselhaus, Science 286 (1999) 1127.
[9] C.Y. Liu, A.J. Bard, F. Wudl, I. Weitz, J.R. Heath, Electrochem. Solid-State Lett. 2 (1999) 577.
[10] J.S. Ye, X. Liu, H.F. Cui, W.D. Zhang, F.S. Sheu, T.M. Lim, Electrochem. Commun. 7 (2005) 249.
[11] J.J. Gooding, Electrochim. Acta 50 (2005) 3049.
[12] A.S. Adekunle, K.I. Ozoemena, J. Solid State Electrochem. 12 (2008) 1325.
[13] M. Musameh, J. Wang, A. Merkoci, Y. Lin, Electrochem. Commun. 4 (2002) 743.
[14] Z. Wang, Q. Liang, Y. Wang, G. Luo, J. Electroanal. Chem. 540 (2003) 129.
[15] F.H. Wu, G.C. Zhou, X.W. Wei, Electrochem. Commun. 4 (2002) 690.
[16] J. Wang, M. Mosameh, Y. Lin, J. Am. Chem. Soc. 125 (2003) 2408.
[17] K.I. Ozoemena, J. Pillay, T. Nyokong, Electrochem. Commun. 8 (2006) 1391.
[18] J. Pillay, K.I. Ozoemena, Electrochim. Acta 52 (2007) 3630.
[19] B.S. Sherigara, W. Kutner, F. D'Souza, Electroanalysis 15 (2003) 753.
[20] A. Salimi, C.E. Banks, R.G. Compton, Analyst 129 (2004) 225.
[21] V. Selvaraj, M. Alagar, K. Sathish Kumar, Appl. Catal., B: Environ. 75 (2007) 129.
[22] A.S. Adekunle, K.I. Ozoemena, Electrochim. Acta 53 (2008) 5774.
[23] M. Yang, Y. Yang, Y. Liu, G. Shen, R. Yu, Biosens. Bioelectron. 21 (2006) 1125.
[24] D.G. Rickerby, M. Morrison, Sci. Technol. Adv. Mater. 8 (2007) 19.
[25] R.P. Deo, N.S. Lawrence, J. Wang, Analyst 129 (2004) 1076.
[26] A. Salimi, E. Shariffi, A. Noorbakhsh, S. Soltanian, Biosens. Bioelectron. 22 (2007) 3146.
[27] A.S. Adekunle, J. Pillay, K.I. Ozoemena, Electroanalysis 20 (2008) 2587.
[28] E. Villagra, F. Bedioui, T. Nyokong, J.C. Canales, M. Sancy, M.A. Paez, J. Costamagna, J.H. Zagal, Electrochim. Acta 53 (2008) 4883.
[29] M. Vidotti, M.R. Silva, R.P. Salvador, S.I. Cordoba de Torresi, L.H. Dall'Antonia, Electrochim. Acta 53 (2008) 4030.
[30] C. Ding, F. Zhao, M. Zhang, S. Zhang, Bioelectrochemistry 72 (2008) 28.
[31] N. Sehlotho, S. Griveau, N. Ruille, M. Boujtita, T. Nyokong, F. Bedioui, Mater. Sci. Eng., C 28 (2008) 606.
[32] J. Arguello, H.A. Magosso, R. Landers, Y. Gushikem, J. Electroanal. Chem. 617 (2008) 45.
[33] A. Salimi, R. Hallaj, H. Mamkhezri, S.M.T. Hosaini, J. Electroanal. Chem. 619 (2008) 31.
[34] A. Salimi, H. Mamkhezri, R. Hallaj, S. Soltanian, Sens. Actuators, B 129 (2008) 246.
[35] M.D. Abad, J.C. Sánchez-López, A. Berenguer-Murcia, V.B. Golovko, M. Cantoro, A.E.H. Wheatley, A. Fernández, B.F.G. Johnson, J. Robertson, Diamond Relat. Mater. 17 (2008) 1853.
[36] Z. Dong, K. Ma, J. He, J. Wang, R. Li, J. Ma, Mater. Lett. 62 (2008) 4059.
[37] M. Yang, J. Jiang, Y. Yang, X. Chen, G. Shen, R. Yu, Biosens. Bioelectron. 21 (2006) 1791.
[38] J. Shen, Y. Hu, C. Li, C. Qin, M. Ye, Electrochim. Acta 53 (2008) 7276.
[39] H. Zhao, L. Li, J. Yang, Y. Zhang, Electrochem. Commun. 10 (2008) 1527.
[40] C.A. Claudia, F. Bedioui, J.H. Zagal, Electrochim. Acta 47 (2002) 1489.
[41] A. Alonso, B. Etxaniz, M.D. Martinez, Food Addit. Contam. 9 (1992) 111.
[42] N. Sparatu, T.N. Rao, D.A. Tryk, A. Fujishima, J. Electrochem. Soc. 148 (2001) E112.
[43] H.J. Choi, G. Kwag, S. Kim, J. Electroanal Chem. 508 (2001) 105.
[44] D.H. Coleman, R.E. White, D.T. Hobbs, J. Electrochem. Soc. 142 (1995) 1152.
[45] J.O'.M. Bockris, A.K.N. Reddy, Modern Electrochemistry, Plenum Press, New York, 1970, p. 1276.
[46] A.L. Leninger, D.L. Nelson, M.M. Cox, Principles of Biochemistry, 2nd ed., Worth Publishers, New York, 1993, p. 689.
[47] S.Y. Ha, S. Kim, J. Electroanal. Chem. 468 (1999) 131.
[48] Z.H. Wen, T.F. Kang, Talanta 62 (2004) 351.
[49] C. Yang, Q. Lu, S. Hu, Electroanalysis 18 (2006) 2188.
[50] J.A. Liu, G. Rinzler, H. Dai, J.H. Hanfer, R.K. Bradley, P.J. Boul, A. Lu, T. Iverson, K. Shelimov, C.B. Huffman, F.R. Macias, Y.S. Shon, T.R. Lee, D.T. Colbert, Science 280 (1998) 1253.
[51] D. Giovanelli, N.S. Lawrence, S.J. Wilkins, L. Jiang, T.G.J. Jones, R.G. Compton, Talanta 61 (2003) 211.
[52] A. Salimi, E. Shariffi, A. Noorbakhsh, S. Soltanian, Biophys. Chem. 125 (2007) 540.
[53] A. Salimi, E. Shariffi, A. Noorbakhsh, S. Soltanian, Electrochem. Commun. 8 (2006) 1499.
[54] J. Zagal, M. Paez, A.A. Tanaka, J.R. dos Santos Jr., C.A. Linkous, J. Electroanal. Chem. 339 (1992) 13.
[55] S. Zecevic, B. Simic-Glavaski, E. Yeager, A.B.P. Lever, P.C. Minor, J. Electroanal. Chem. 196 (1985) 339.
[56] A.B.P. Lever, S. Liccocia, K. Magnell, P.C. Minor, B.S. Ramaswamy, Am. Chem. Sot. Symp. Ser. 201 (1982) 237.
[57] A. Salimi, R. Hallaj, S. Soltanian, H. Mamkhezri, Anal. Chim. Acta 594 (2007) 24.
[58] S. Sunohara, K. Nishimura, K. Yahikozawa, M. Ueno, J. Electroanal. Chem. 354 (1993) 161.
[59] User Manual for Frequency Response Analysis (FRA) for Windows version 4.9, Eco Chemie B.V., Utrecht, The Netherlands, 200 (and references therein).
[60] B.A. Boukamp, J. Electrochem. Soc. 142 (1995) 1885.
[61] G. Nurk, H. Kasuk, K. Lust, A. Janes, E. Lust, J. Electroanal. Chem. 553 (2003) 1.
[62] H. Kasurk, G. Nurk, E. Lust, J. Electroanal. Chem. 613 (2008) 80.
[63] W. Lajnef, J.-M. Vinassa, S. Azzopardi, O. Briat, E. Woirgard, C. Zardini, J.L. Aucouturier, PESC 04 1 (2004) 131.
[64] V. Ganesh, S. Pitchumani, V. Lakshminarayanan, J. Power Sources 158 (2006) 1523.
[65] M.E. Orazem, B. Tribollet, Electrochemical Impedance Spectroscopy, John Wiley & Sons Inc., Hoboken, NJ, 2008 (Chapter 13).
[66] M. Thamae, T. Nyokong, J. Electroanal. Chem. 470 (1999) 126.
[67] P. Tau, T. Nyokong, Electrochim. Acta 52 (2007) 4547.
[68] F. Matemadombo, T. Nyokong, Electrochim. Acta 52 (2007) 6856.
[69] B.O. Agboola, T. Nyokong, Anal. Chim. Acta 587 (2007) 116.
[70] J. Bisquert, H. Randriamahazaka, G. Garcia-Belmonte, Electrochim. Acta 51 (2005) 627–640.
[71] M. Jafarian, M.G. Mahjani, H. Heli, F. Gobal, H. Khajehsharifi, M.H. Hamedi, Electrochim. Acta 48 (2003) 3423.
[72] S. Majdi, A. Jabbari, H. Heli, A.A. Moosavi-Movahedi, Electrochim. Acta 52 (2007) 4622.
[73] A.J. Bard, L.R. Faulkner, Electrochemical Methods: Fundamentals and Applications, 2nd ed., John Wiley & Sons, Hoboken, NJ, 2001.
[74] J.N. Soderberg, A.C. Co, A.H.C. Sirk, V.I. Birss, J. Phys. Chem. B 110 (2006) 10401.
[75] R. Ojani, J.-B. Raoof, E. Zarei, Electrochim. Acta 52 (2006) 756.
[76] N.S. Trofimova, A.Y. Safronov, O. Ikeda, Electrochim. Acta 50 (2005) 4637.
[77] G.D. Christian, Analytical Chemistry, 6th ed., John Wiley and Sons, New York, 2004, p. 113.
[78] K.I. Ozoemena, Z. Zhao, T. Nyokong, Inorg. Chem. Commun. 9 (2006) 223.
[79] E. Casero, J. Losada, F. Pariente, E. Lorenzo, Talanta 61 (2003) 61.
[80] H.X. Ju, L. Donal, J. Electroanal. Chem. 484 (2000) 150.
[81] F. Armijo, M.C. Goya, M. Reina, M.J. Canales, M.C. Arevalo, M.J. Aguire, J. Mol. Catal. A 268 (2007) 148.

Please cite this article in press as: A.S. Adekunle, et al., Probing the electrochemical behaviour of SWCNT–cobalt nanoparticles and their electrocatalytic activities towards the detection of nitrite at acidic and physiological pH conditions, Electrochim. Acta (2009), doi:10.1016/j.electacta.2009.02.102